Fast-running tool dedicated to power excursion simulations in sodium-cooled fast reactor

K. Herbreteau, N. Marie, F. Bertrand, J.-M. Seiler, P. R. Rubiolo

FAST-RUNNING TOOL DEDICATED TO POWER EXCURSION SIMULATIONS IN SODIUM-COOLED FAST REACTOR

K. Herbreteau, N. Marie, F. Bertrand
CEA, DEN, DER, SESI, F-13108, Saint Paul lez Durance, France
kevin.herbreteau@cea.fr; nathalie.marie@cea.fr; frederic.bertrand@cea.fr

J-M. Seiler
CEA, DEN, DTN, STCP, F-13108, Saint Paul lez Durance, France
jean-marie.seiler@cea.fr

P. Rubiolo
CNRS, IN2P3, LPSC, F-38054, Grenoble, France
pablo.rubiolo@lpsc.in2p3.fr

ABSTRACT

Within the framework of the Generation IV Sodium-cooled Fast Reactor (SFR) within the CEA (French Commissariat à l'Energie Atomique et aux Energies Alternatives) is involved, the innovative reactor designs under severe accidents conditions have to be assessed. Such accidents have been mainly simulated with mechanistic calculation tools (such as SAS and SIMMER). As a complement to these codes, which provide reference accidental transients calculations, a new physico-statistical approach is currently developed at CEA; its final objective being to derive the variability of the main results of interest to quantify the safety margin. This approach involves fast-running tools to simulate extended accident sequences, by coupling models of the main physical phenomena with advanced statistical analysis techniques. They enable to perform a large number of simulations in a reasonable computational time and to describe all the possible scenario progressions of the hypothetical accidents. In this context, this paper presents a physical tool (numerical models and result's assessment) dedicated to the simulation of the beginning of the primary phase of the Unprotected Transient OverPower accidents (i.e. before large pin degradation).
At the beginning of this primary phase, the increase of nuclear power induces a strong temperature gradient in the fuel pellets leading to specific mechanical behaviours, such as swelling and thermal expansion, before their meltdown. The fuel pin thermal evolution during slow power increases, such as control rod withdrawal accidents, and fast power increases have been performed. Validation on some CABRI experiments was carried out and focused on the axial distribution of melting points in the fuel column, the molten fraction at the end of the transient and the coolant temperature evolution during the transient. The results are consistent with experimental data and an application case on the CFV core of ASTRID was performed in order to give tracks for the safety of the reactor.

KEYWORDS
Sodium-cooled Fast Reactor, Transient OverPower, Severe Accident, Fast-running tool

1. INTRODUCTION

The current main objective of the French Generation IV project is to design a new reactor based on improved technologies in terms of safety and reliability at an industrial scale. Among other concepts, the Sodium-cooled Fast Reactor (SFR) has been selected for its ability to secure the nuclear fuel resources and to manage radioactive waste by minor actinides transmutation. A major innovation of the new SFR

French concept concerns the core, which is featured by a very low (even negative) reactivity variation caused by a potential sodium voiding. More specifically, this feature has a strong impact on the severe accident sequences especially regarding the material heating-up and on the global core power evolution [1]. In this framework of safety studies devoted to the Unprotected Transient OverPower (UTOP), a physical tool, called OCARINa (Outil de Calcul Analytique Rapide pour les Insertions de réactivité dans un réacteur à neutrons rapides refroidi au sodium), is being developed. As a complement to reference transients which are usually simulated with mechanistic codes such as SIMMER [2], physical tools, coupled to advanced statistical technics, enable to get the variability of the main results of interest for the safety. This general approach combining a mechanistic code and evaluation tools has already been conducted for another accidental initiator family (USAF - Unprotected SubAssembly Fault [3] and ULOF – Unprotected Loss Of Flow [4]).

Up to now, there is no tool dedicated to the simulation of the UTOP transient for heterogeneous cores. The SAS code is used to describe the primary phase (i.e. before large pin degradation) of a severe accident but it cannot handle two molten cavities in the fuel pin for heterogeneous fuel pin and is not able to describe the degradation phase (i.e. after large pin degradation). Moreover, the SIMMER code is currently used to describe the degradation phase but the mechanical models are not able to describe the primary phase. As an example, the fuel axial expansion is not modeled whereas it has a strong negative reactivity effect. These limitations prove that the development of this physical tool fills a gap in severe accident studies.

A focus on the phenomena occurring during UTOP transients are described in section 2. They are modelled in accordance to the level of details required to catch all the decisive phenomena. The physical models used so far (thermal models) are presented in section 3. Their validation against some CABRI experiments and an application on the CFV core are then presented in the same section.

2. UTOP TRANSIENT

Core design is obviously driven by performance and safety objectives. An important design and safety purpose is the prevention of a power excursion in case of sodium voiding. The core concept (called CFV) is an axial heterogeneous core of 1500MWth on the contrary to more classical homogeneous cores used in former SFR. The low sodium void effect of the CFV core mainly results from the presence of a sodium plenum above the fissile zones, combined to the presence of a fertile plate in the inner zone of the core encompassed by two fissile zones (displayed in Figure 1). The larger height of the outer fissile zone also enables the void reactivity effect to be lowered as well, due to neutron leakage enhancement.

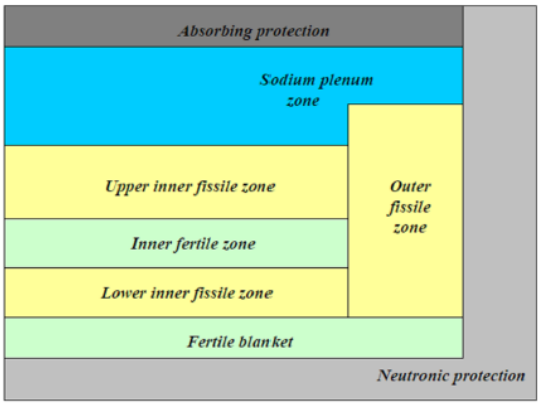

Figure 1. Radial cut of CFV core geometry.

2.1. Different initators

The UTOP is characterized, in the first place, by an external reactivity insertion leading to an increase of the nuclear power. The increase could be local or global with a specific kinetic (slow or fast power variation). Four types of UTOP, according to different initiators, are usually considered:

- **Inadvertent Control-rod Withdrawal (IRW)**

It is the most common transients occurring during reactor operation as they manage the regulation of the core power. In a fast neutron reactor, in such accident, a linear power increase of about 1-3 %PN/s [W/s] (PN stands for the nuclear power on normal conditions) in pins located near the withdrawn control rod could be generated.

- **Compaction of the core**

The reactivity inserted is assumed to have a sinusoidal shape due to a succession of compaction (positive reactivity insertion) and stacking (negative reactivity insertion).

- **Fall of the core**

The fall of the core is assumed to be radially homogenous; all the control-rods are stuck at their mechanisms. The reactivity inserted is therefore equal to the neutronic weight of the control-rods.

- **Gas ingress into the core**

This event may occur due to the entrainment of a part of the cover-gas plenum by the primary pumps that could push the gas into the core. The associated reactivity insertion depends on the size of the bubble and on the location of the bubble. The CFV core has a global negative void effect but it is positive close to the fissile zones.

The aim of the tool is to describe all of those UTOP transients on a reactor scale. Currently, power-imposed transients are modeled considering a single pin.

2.2. Overall phenomenology

Considering any of the previous postulated event, the multi-physic (thermic, mechanic, neutronic) phenomenology remains the same (Figure 2). Due to the fast kinetic of UTOP transient (except power-ramp transients), some physical phenomena have not the time to settle and there is no need to model them such as axial thermal conduction (see section 3).

The main phenomena up to clad failure can be summarized as the following:

1. Reactivity insertion: the core becomes super-critical;
2. The nuclear power increases;
3. The fuel temperature increases, the Doppler effect tends to slow down the power increase;
4. If the Doppler effect isn’t efficient enough to lower the reactivity down to zero, the fuel could melt;
5. The fuel melts in the center of the pellet: a molten cavity is created;
6. The fuel phase change combined with thermomechanical phenomena induces significant mechanical strain in the fuel pin clad;

7. Fuel pin clad failure;
8. Molten fuel is ejected out of the pin into the coolant increased by the eventual fission gas present.

Up to now at the current development stage of the tool, only a simplified sequence is modeled. No neutronic coupling is taking into account: the power variation is imposed during the transient.

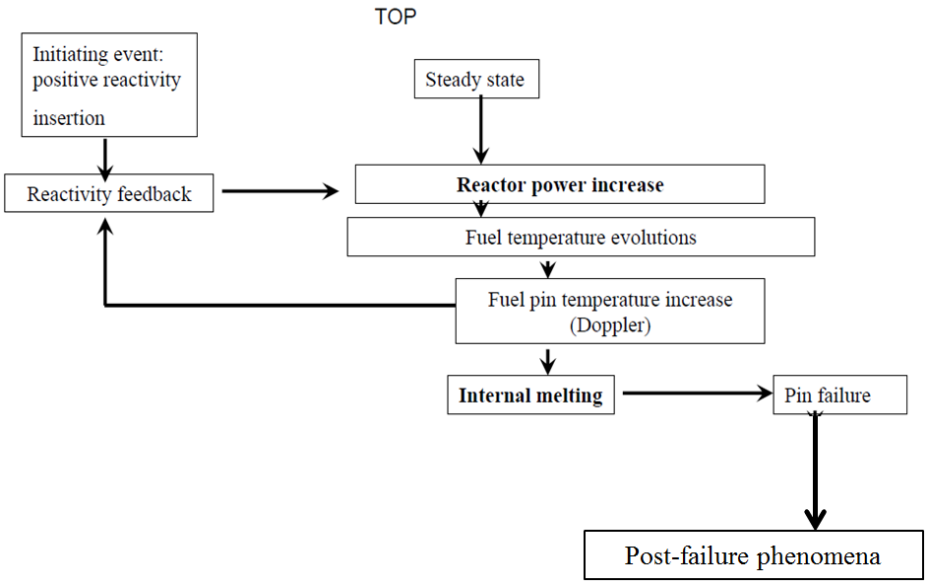

Figure 2. Phenomenology tree of the UTOP transient up to clad failure.

2.3. Few words about CABRI

The CABRI core is a 25MW (Mega-Watt) thermal nuclear reactor operating with LWR-like fuel. The test channel is in the center of the core. The power transients are triggered with transient rods filled with gaseous Helium-3. Fast depressurization of these rods leads to a reactivity insertion in the core and a power transient up to 20GW (Giga-Watt).

3. PHYSICAL MODELS

The UTOP transient is characterized by fuel heating-up to its possible melting. Thus, a two-dimensional meshing of the pin is considered the most reasonable for an accurate simplified simulation in order to take into account the evolution if the fuel property versus the temperature which have been evidenced having an influence on the transient, especially through the thermal conductivity of the fuel [5]. The sodium flow is considered as unidirectional from the bottom (inlet) to the top (outlet). Variables related to sodium and to the wrapper are space-averaged over each axial mesh as illustrated in Figure 3.

One or several subassemblies of the reactor core are modeled by a representative subassembly (noted SA) including the pins, its sodium coolant flow and its surrounding hexagonal wrapper (as done in SAS-SFR [6]). For example, for a single CABRI pin geometry, the pin modeled is presented in Figure 4.

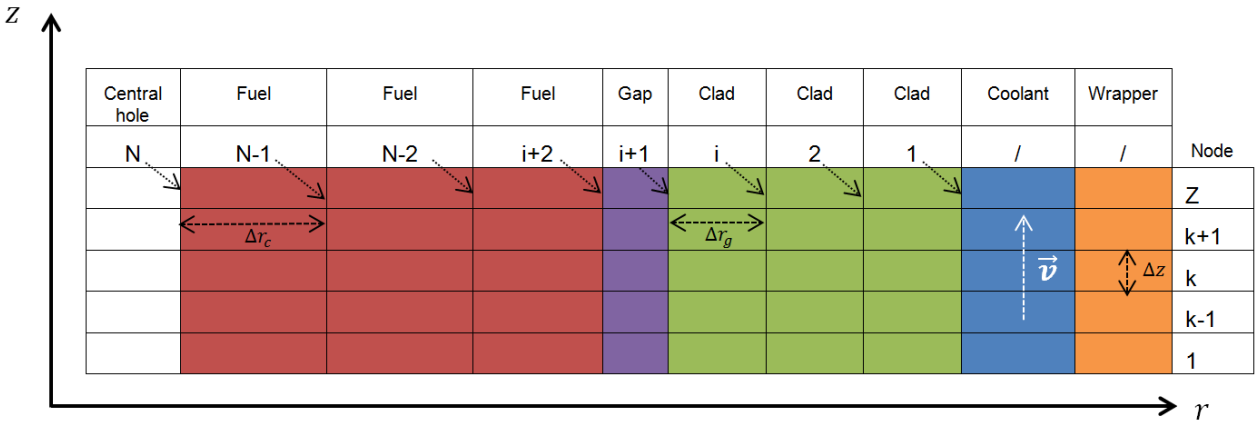

Figure 3. 2D meshing used for the modeling.

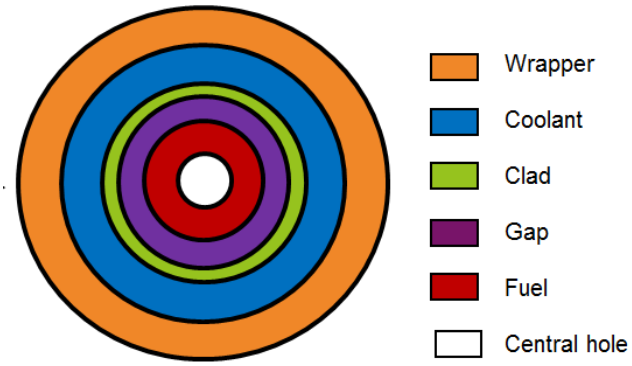

Figure 4. Axial cut of a subassembly (or a single pin in the CABRI channel).

3.1 Thermal modeling

The knowledge of the temperature in the fuel, the clad and the coolant is a mandatory step for the transient modeling. In fact, the temperature has an impact on the mechanical evolution of the fuel (thermal expansion, phase change, strains, creeps etc.) and on the nuclear power evolution via the Doppler effect. A finite difference method is used with an implicit coupling between the temperature of the sodium and the temperature in the fuel/clad [7]. The coupling is made with the flux exchanged between the sodium and the clad. Many UTOP transients are very fast and require an unconditional stable numerical scheme. That's why a completely implicit numerical scheme has been developed. An explicit numerical scheme has been tested (the coupling is made with the flux exchanged between the sodium and the clad at the previous time step) and was not stable for fast transients.

3.1.1 Equations

The energy balances used are:

- One-dimensional radial heat transfer in the fuel:

$$\left(\rho C_p\right)_f \frac{\partial T_f}{\partial t} = \mathrm{div}\left(k_f \overrightarrow{\mathrm{grad}}\, T_f\right) + q''' \quad (1)$$

- One-dimensional radial heat transfer in the clad:

$$\left(\rho C_p\right)_{cd} \frac{\partial T_{cd}}{\partial t} = \mathrm{div}\left(k_{cd} \overrightarrow{\mathrm{grad}}\, T_{cd}\right) \quad (2)$$

- One-dimensional axial energy balance in the coolant (liquid phase only):

$$\frac{\partial \rho_c H_c}{\partial t} + \frac{\partial G_c H_c}{\partial z} = \frac{2\pi}{S_c}\left(r_{cd}\varphi_{cd} + r_w\varphi_w\right) \quad (3)$$

- Energy balance of the wrapper:

$$\left(\rho C_p V\right)_w \frac{\partial T_w}{\partial t} = -S_w\varphi_w \quad (4)$$

Where ρ, C_p, k, T stand respectively for density [kg/m^3], specific heat [J/kg/K], thermal conductivity [W/m/K] and temperature [K] of the fuel (f), the clad (cd), the coolant (c) and the wrapper (w).

In equation (1), q''' stands for the volumetric power source of the fuel [W/m^3]. At each time step, it is actualized depending on the imposed transient power.

Then in equation (3), H_c, G_c, S_c, r_{cd}, φ_{cd}, r_w, φ_w stand respectively for the coolant enthalpy [J/kg], the coolant flow rate [kg/m^2/s], the flow cross section [m^2], the outer radius of the clad [m], the heat flux exchange between the clad and the coolant [W/m^2], the inner radius of the wrapper [m] and the heat flux exchange between the coolant and the wrapper [W/m^2].

Finally in equation (4), V_w and S_w stand for the control volume of wrapper [m^3] and the exchange surface between the coolant and the wrapper [m^2].

Due to the kinetic of the transient and regarding the characteristic time of axial conduction in the fuel and the clad defined by:

$$\tau_{\text{axial conduction}} = \frac{\rho C_p}{k} L^2$$

Where L stands for a characteristic length of the medium (two pellets for the fuel, the same value for the clad), it leads to a characteristic time of axial conduction (~10^5 s) much higher than the transient time (~10^{-3} s for fast transient to 100 s for power ramps). That is why the axial conduction in the fuel and the clad are neglected.

3.1.2 Boundary conditions

An axisymmetric condition and an adiabatic condition beyond the wrapper are taken as boundary conditions.

The heat exchange between the fuel and the clad through the gap is described by a global heat exchange coefficient h_{gap} [W/m^2/K]. Concerning the CABRI tests, its value depends on the kinetic of the transient. For slow transient, the value $h_{gap} = 10^4$ W/m^2/K is taken and it corresponds to an average value determined by a GERMINAL calculation [8]. For fast transients, the value $h_{gap} = \infty$ (in practice 10^9 W/m^2/K) is taken, corresponding to a perfect solid contact between the pellet and the clad. It is justified

by the resulting fast increase of the pellet temperatures which make the solid contact quasi-instantaneous by thermal expansion and phase change.

Finally, the heat exchange between the clad and the sodium is given by the Lyon-Martinelli [9] transfer correlation:

$$\mathrm{Nu} = 7 + 0.025\mathrm{Pe}^{0.8}$$

Where Nu and Pe stand for Nusselt and Peclet numbers.

3.1.3 Numerical resolution and analysis

After discretization, the energy balance equations and the boundary conditions provide a tridiagonal linear system per axial mesh:

$$\mathrm{MT} = \mathrm{v}$$

With T stands for the unknown vector containing the temperature of every node in an axial mesh (fuel, clad, coolant and wrapper), v stands for a known vector and M is a tridiagonal matrix. The inversion of the matrix is assured with the Thomas algorithm [10]. Moreover, in order to provide an accurate result at each matrix inversion, a numerical analysis was performed focusing on:

- the condition number $\kappa(\mathrm{M})$ defined, under the Frobenius norm [11], by the ratio between the highest and the lowest eigen values of the matrix. For a well-conditioned matrix, $\kappa(\mathrm{M}) = 1$;
- the residual error, defined by $\mathrm{r} = |\mathrm{v} - \mathrm{MT}|$, must be negligible.

The block diagram of the thermal resolution is shown in Figure 5. It begins with a steady state calculation followed by the transient calculation. The thermal properties are calculated with the temperature at the previous time step because at the current time step, the temperature in unknown. That's why a convergence loop is used to keep the implicit numerical scheme even on solid properties.

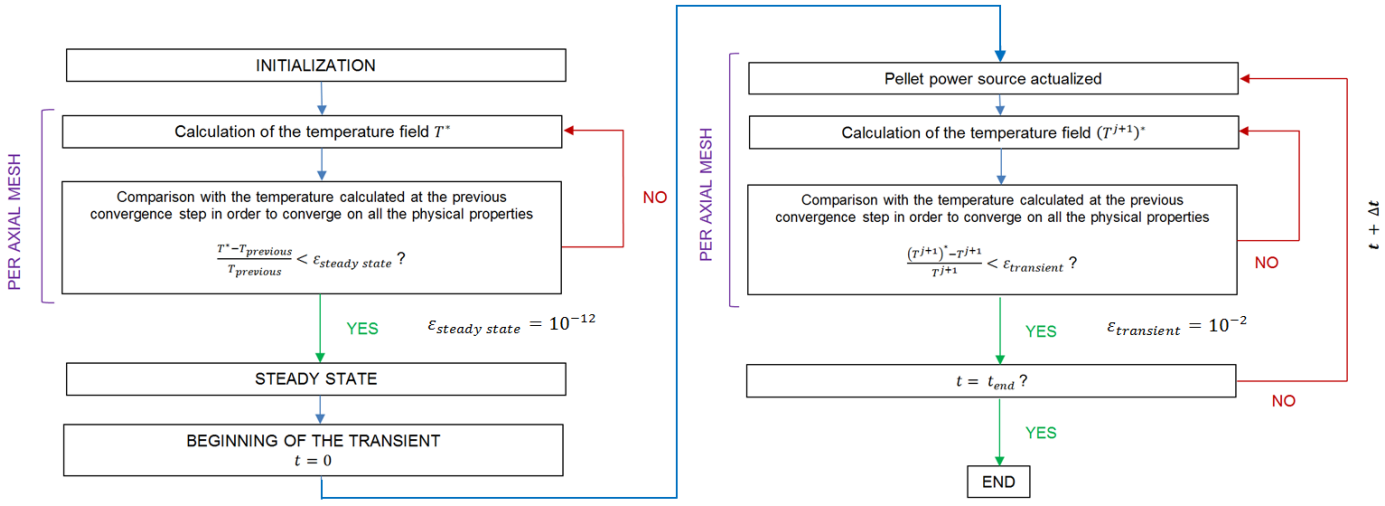

Figure 5. Block diagram of the thermal resolution.

3.2 Validation of the thermal modeling

This numerical scheme was testes on six CABRI tests [12], [13], [14]. Four fast transients: E5, E7, LT2, AGS0 and two slow transients: PF1, E9 (Table I). All the results are summarized in the same Table I. Some results obtained for fast transients (E5) and one slow transient (PF1) are shown in Figure 6 and 7. The unvalidated results (Table I) are also shown in Figure 8. Globally, the thermal modeling gives good agreements with experimental data inside the uncertainty ranges so the model is considered validated regarding the objectives of the physical tool. It shows that the heat-up of all the medium during a power excursion can be accurately described with a simplified model.

However, the differences with experimental data for the E9-test can be explained by the lack of mechanical modeling during the transient. Indeed, the evolution of the pellet-clad exchange coefficient is not yet modeled in the physical tool (see section 3.1.2). The average value taken for the whole transient must be better for the PF1 test than the E9 test, which could explain why good results are obtained for the PF1 test. Anyhow, the pellet-clad exchange coefficient evolution during the transient constitutes one of the following steps of modeling.

Table I. Validation database used for the thermal modeling.
(P_{max} – Maximum power, P_0 – Power at steady state, t_{Pmax} – Time of the power peak)
(V – Validated (see the section above), NA – Data not available, NV – Not yet validated)

Transient	**E5**	**E7**	**LT2**	**AGS0**	**PF1**	**E9**
Type	TOP	TOP	TOP	TOP	Power ramp	Power ramp
$\frac{P_{max}}{P_0}$ (t_{Pmax})	26 (320ms)	200 (450ms)	26 (600ms)	11 (400ms)	2,2 (90s)	2,3 (120s)
Pin burn-up (at%)	5	4,6	12,4	2,9	6,4	4,6
Pin design	OPHELIE-6 (annular)	OPHELIE-6 (annular)	QUASAR (solid)	RIG-2 (solid)	SCARABIX (annular)	OPHELIE-6 (annular)
Condition number κ	~ 1	~ 1	~ 1	~ 1	< 5	< 4
Residual error r	$< 2{,}5.10^{-4}$	$< 2{,}5.10^{-4}$	$< 2{,}5.10^{-4}$	$< 2{,}5.10^{-4}$	$< 6.10^{-8}$	$< 6.10^{-8}$
Coolant temperature at steady state	**V**	**V**	**V**	*NA*	*NA*	**V**
Coolant temperature at the power peak	*NA*	**V**	*NA*	**V**	*NA*	*NA*

Table I. Validation database used for the thermal modeling.
(P_{max} – Maximum power, P_0 – Power at steady state, t_{Pmax} – Time of the power peak)
(V – Validated (see the section above), NA – Data not available, NV – Not yet validated)

Coolant temperature at the top fissile colum	**V**	*NA*	**V**	*NA*	**V**	**V**
Molten radius	**V**	*NA*	**V**	**V**	**V**	NV

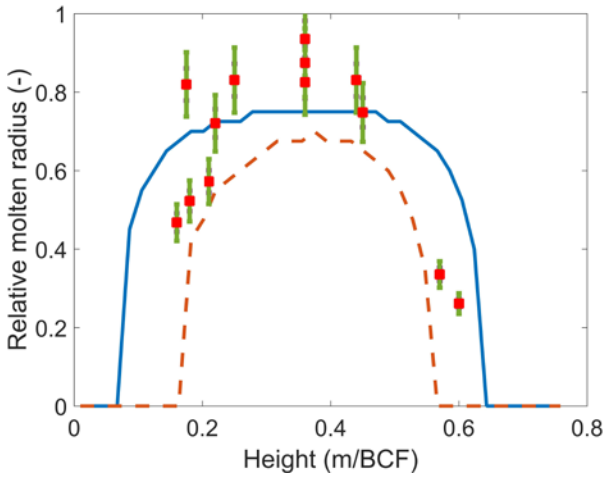

Figure 6. Molten radius for E5 transients (Solidus front – solid, Liquidus front – dotted, Experimental double-phase front – squared). The fuel is in a double-phase state between the solidus and the liquidus front.

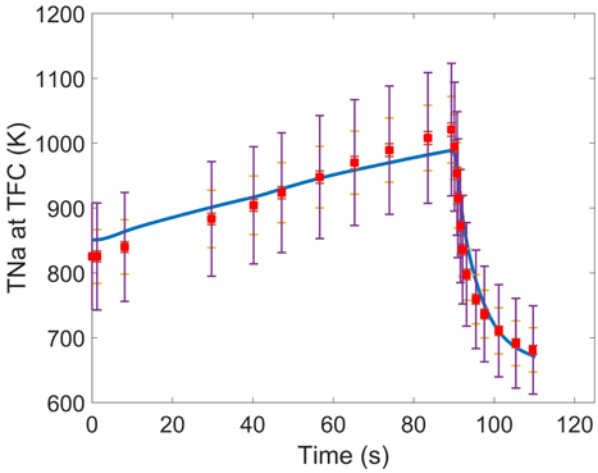

Figure 7. Evolution of the Top Fuel Column (TFC) sodium temperature during PF1 transient (Experimental data – squared).

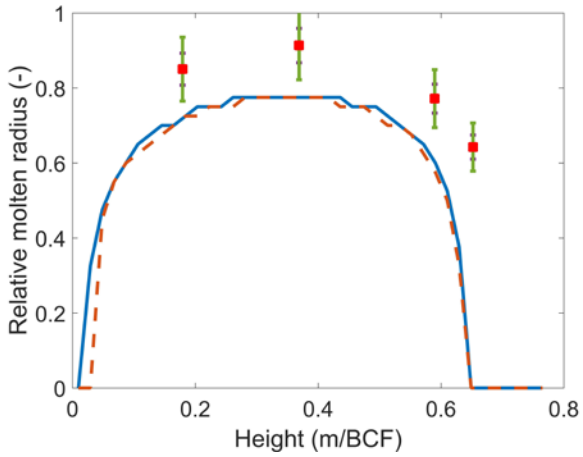

Figure 8. Molten radius for E9 transients (Solidus front – solid, Liquidus front – dotted, Experimental double-phase front – squared). The fuel is in a double-phase state between the solidus and the liquidus front.

3.3 Application on the CFV design

UTOP power-imposed simulations have been performed focusing on an inner CFV core subassembly, described in Figure 9.

The idea is to suppose that a CFV inner core pin was inserted into the CABRI core. The same power evolution as E5 and E7 transients (Figure 10) are imposed. The linear power distribution at steady state is exposed on Figure 11.

Core design	CFV-V3
Nominal thermal power [MW]	1500
Inner fissile zone height [cm]	25 + 35
Outer fissile zone height [cm]	90
Inner fertile zone height [cm]	20
Inner zone radius [cm]	133.5
Outer zone radius [cm]	162.6
Sub-assembly pitch [cm]	17.5
Fissile zones PuO_2 enrichment(inner/outer) [%volumic]	20/23
Effective delayed neutron fraction (β_{eff}) [pcm]	364
Void reactivity effect ($) Core at equilibrium	−0.5

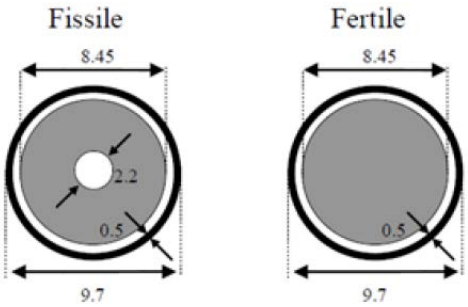

Figure 9. CFV subassembly features [3].

Due to the lack of neutronic and mechanic modeling, it is assumed in a first approximation that there is no modification of the axial form factor of the neutron flux during the transient like in CABRI. The linear power distribution magnitude is updated during the transient depending on the power evolution. At each time step, the linear power $q'(z,t)$ is equal to:

$$q'(z,t) = q'(z,t_0)\, P_{relative}(t)$$

Where $q'(z,t_0)$ stands for the linear power at the beginning of the transient and $P_{relative}(t)$ stands for the relative power evolution (Figure 11).

It has to be noted that the power evolution of the CABRI core was set regarding the energy per unit of mass injected into the fuel. The power integrated of a CFV pin is lower than pins used for E5 and E7 transients due to the fertile zones. So the energy injected into the CFV pin is lower than the energy injected into the CABRI pins and the results can't be directly compared.

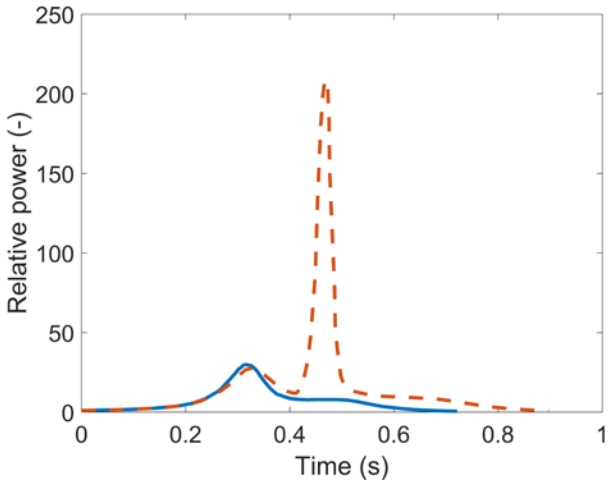

Figure 10. Relative power evolution imposed during the transient (E5 – solid, E7 – dotted).

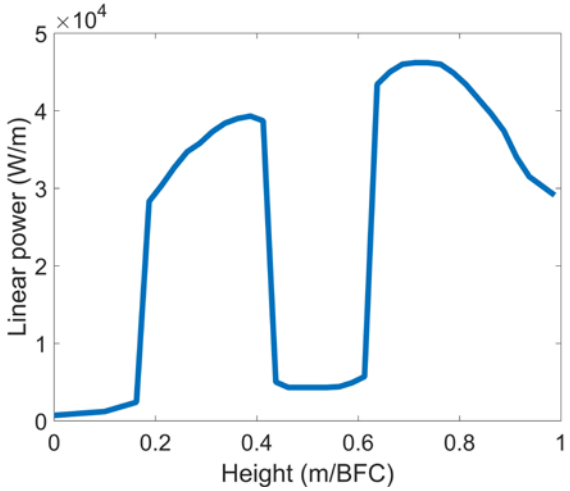

Figure 11. Linear power axial distribution at steady state (inner core, BFC – Bottom of the Fuel Column).

Regarding the heat exchange coefficient between the fuel and the clad through the gap, a constant value was taken for the fertile zones and another one for the fissile zones. Those values were provided by another GERMINAL calculation [8].

The results obtained for the sodium temperature at the Top of the Fuel Column (TFC) show (Figure 12) that for E5-like transient, there is a good margin regarding sodium boiling (around 250K). Also for E7-like transient, there is a margin regarding sodium boiling but a smaller one (around 50K). Due to the lower energy injected into the pin, it is not guarantee that sodium boiling do not appear for the same energy injected as the CABRI tests.

Now focusing on the molten radius at the power peak (Figure13), the E5-like transient leads to small amount of molten fuel in the upper fissile zone (less than 1% of the total volume of fuel). It means that it may not be axial motion of molten fuel through the pin according to previous experimental data [15] and the central hole could be efficient enough to decrease strains on the clad and avoid its failure [16].

On the contrary, E7-like transient leads to 30% of molten fuel in the pin with more than 80% of molten fuel in the upper fissile zone. This amount allows axial motions considering the experimental criteria of 40% of molten fuel used in the PHYSURA code [17]. Due to the solid pellets constituting the fertile zones, the molten fuel cannot flow through the central hole by gravity flow or squirting effect [16], preventing the release of strains on the clad. In that configuration, the clad will endure strong stresses and may break. Moreover, the melting pools surrounding the inner fertile zone could lead to the collapse of the fertile pellets.

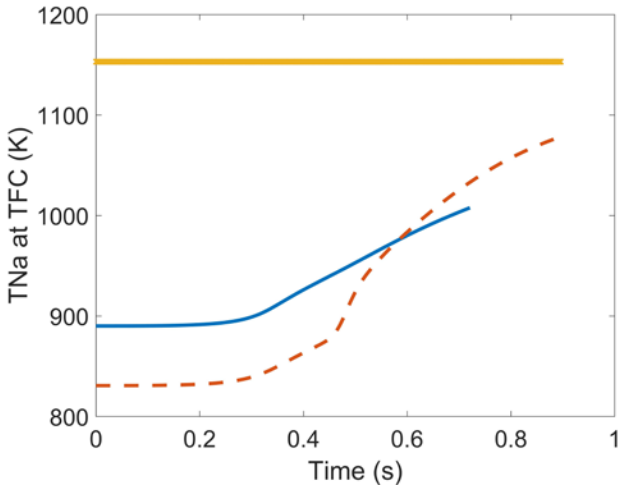

Figure 12. Evolution of the Top Fuel Column (TFC) sodium temperature during the transient (E5 – solid, E7 – dotted, Boiling temperature = 1153K at 1 bar).

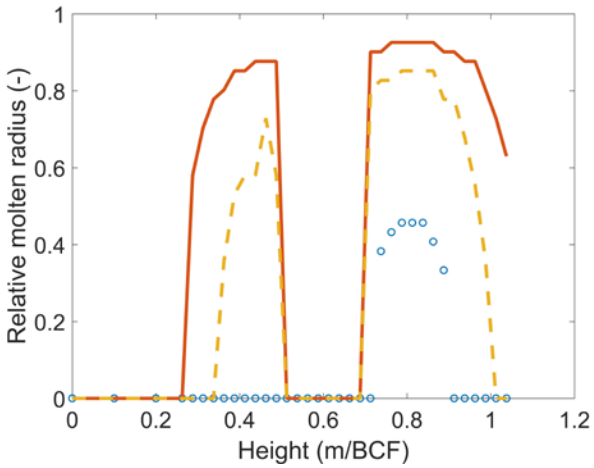

Figure 13. Melting radius at the power peak
(Solidus front E7 – solid, Liquidus front E7 – dotted, Solidus front E5 – circled, no liquidus front E5). The fuel is in a double-phase state between the solidus and the liquidus front.

Those conclusions have to be confirmed simulating as well thermomechanical modeling of the fuel and the clad.

4. CONCLUSION

This paper deals with the preliminary development of a physical tool which will be used for safety-informed design and to address core melting prevention and mitigation situations of sodium-cooled fast reactors. This tool will allow emphasizing main dominant phenomena and trends of significance for safety assessment. It is more specifically dedicated to the primary phase of an Unprotected Transient OverPower (i.e. before large pin degradation) in a heterogeneous core for which none adequate tool exist. This study focuses on the modeling, validation on CABRI experiments and an application on the CFV core of the heat-up of the fuel, clad, coolant and the wrapper up to large fuel fusion. The modeling of this tool is described. At that stage, it handles challenging implicit coupled resolution of:

- a one-dimensional transient heat equation in the solid materials of the SA (or single pin);
- a one-dimensional energy balance on the sodium flow along the SA height (one-phase flow modeling) and on the wrapper.

Validation against experiments has been performed using CABRI experimental database. It provided good results, especially regarding the coolant temperature evolution and the molten radius along the pin. It shows that the thermal evolution of the fuel, the clad and the coolant during a power excursion are accurately described with those analytical models. Two realistic power transients were then imposed on a CFV inner core and it gives tracks for the following steps of modeling such as sodium boiling and the collapse of the inner fertile zone.

The forthcoming work will focus on the thermomechanical modeling of the fuel and the clad. Indeed, most of mechanical phenomena occurring during a UTOP transient are thermal activated such as the thermal expansion of the fuel its expansion when it melts. Such phenomena will induce strong stresses on the clad and could lead to its failure. Its prediction (height of the failure and the failure time during the transient) therefore constitutes the main next step of modeling.

REFERENCES

1. F. Bertrand, N. Marie, G. Prulhiere, J. Lecerf, and J.M. Seiler, “Comparison of the behavior of two core designs for ASTRID in case of severe accidents”, *Nuclear Engineering and Design*, Vol. 297, pp 327-342 (2015).
2. S. Kondo, K. Morita, Y. Tobita, K. Kamiyama, D.J. Brear, and E.A. Fischer, “SIMMER-III : computer program for LMFR core disruptive accident analysis”, O-arai Engineering Center, Power Reactor and Nuclear Fuel Development Corporation (1996).
3. N. Marie, A. Marrel, J.M. Seiler, and F. Bertrand, “Physico-statistical approach to assess the core damage variability due to a Total Instantaneous Blockage of SFR fuel sub-assembly”, *Nuclear Engineering and Design*, Vol. 297, pp 343-353 (2016).
4. J.B. Droin, “Modélisation du transitoire ULOF”, PhD thesis, Université de Grenoble Alpes (2016).
5. Y. Philipponneau, “Thermal conductivity of $(U,Pu)O_{2-x}$ mixed oxide fuel”, *Journal of Nuclear Material*, Vol. 188, pp 194-197 (1992).
6. D. Lemasson and F. Bertrand, “Simulation with SAS-SFR of a ULOF transient on ASTRID- like core and analysis of molten clad relocation dynamics in heterogeneous subassemblies with SAS- SFR, *ICAPP'14*, Charlotte, USA (2014).

7. A. Latrobe, “A comparison of some implicit finite difference schemes used in flow boiling analysis”, *In Proceedings of OECD specialists meeting on two-phase flows*, Toronto, Canada (1976).
8. J.C. Melis, L. Roche, J.P. Piron and J. Truffert, “GERMINAL – A computer code for predicting fuel pin behavior”, *Journal of Nuclear Materials*, Vol. 188, pp 303-307 (1992).
9. F. Agosti and L. Luzzi, “Heat Transfer Correlations for Liquid Metal Cooled Fast Reactors – Short Handbook”, Politecnico di Milano - Department of Nuclear Engineering (2007).
10. L.H. Thomas, “Elliptic Problems in Linear Differential Equations over a Network”, Watson Sci. Comput. Lab Report, Columbia University, New York (1949).
11. G.H. Golub, C.F Van Loan, “Matrix computation, 3rd edition”, Baltimore, MD Johns Hopkins (1996).
12. M. Cranga and all. "Transient material behaviour in CABRI-1 experiment failure under fully and semi-restrained fuel pin conditions." Vol.l, p. 421 International Fast Reactor Safety Meeting, SNOWBIRD, August (1990).
13. M. Haessler et al., “The CABRI-2 Programme—Overview on Results,” Proc. Int. Fast Reactor Safety Mtg., Snowbird, Utah, August 12–16, 1990, Vol. II, p. 209, American Nuclear Society (1990).
14. Y. Fukano, Y. Onoda, I. Sato and J. Charpenel, “Fuel pin behavior under slow ramp-type transient-overpower conditions in the CABRI-FAST experiments”, *In Proceedings of 13th International Topical Meeting on Nuclear Reactor Thermal Hydraulics (NURETH13)*, Kanzawa City, Ishikawa Prefecture, Japan, Septembre 27 – October 2 (2009).
15. J. Papin, “Behavior of Fast Reactor Fuel During Transient and Accident Conditions”, *Comprehensive Nuclear Materials, 2012, Elsevier Ltd* (2012).
16. “Le code PHYSURA, Objectifs, Description et Validation”, Cadarache nuclear study center, CEA report CEA-R-5200, http://www.iaea.org/inis/collection/NCLCollectionStore/_Public/15/001/15001924.pdf (1983).
17. I. Sato, U. Imke, W. Pfrang, M. Berne, “Transient fuel pin behaviour and failure conditions in CABRI-2 in-pile tests”, *In Proceedings of International Topical Meeting on Sodium Cooled Fast Reactor Safety*, Obninsk, Russia, Oct 3–7 1994, Vol. 2, pp 134 (1994).